

Wildfire Resilient Unit Commitment under Uncertain Demand

Ryan Greenough, Kohei Murakami, Michael Davidson, Jan Kleissl, and Adil Khurram

Abstract—Public safety power shutoffs (PSPS) are a common pre-emptive measure to reduce wildfire risk due to power system equipment. System operators use PSPS to de-energize electric grid elements that are either prone to failure or located in regions at a high risk of experiencing a wildfire. Successful power system operation during PSPS involves coordination across different time scales. Adjustments to generator commitments and transmission line de-energizations occur at day-ahead intervals while adjustments to load servicing occur at hourly intervals. Generator commitments and operational decisions have to be made under uncertainty in electric grid demand and wildfire potential forecasts. This paper presents deterministic and two-stage mean-CVaR stochastic frameworks to show how the likelihood of large wildfires near transmission lines affects generator commitment and transmission line de-energization strategies. The optimal costs of commitment, operation, and lost load on the IEEE 14-bus test system are compared to the costs generated from prior optimal power shut-off (OPS) formulations. The proposed mean-CVaR stochastic program generates less total expected costs evaluated with respect to higher demand scenarios than costs generated by risk-neutral and deterministic methods.

Index Terms—Public Safety Power Shut-offs, optimal power flow, extreme weather event, day-ahead unit commitment & wildfire risk mitigation

I. INTRODUCTION

Since 2012, an important short-term strategy for electric utilities to proactively reduce wildfire ignition probabilities is public safety power shut-offs (PSPS) [1]–[3]. A PSPS seeks to ensure reliable electrical grid operation during wildfires [2] and maximize load served while minimizing wildfire risk. In [4], a significant increase in PSPS is predicted due to drier autumn seasons in California’s future. Across the US, the annual wildfire frequency is predicted to increase by 14% by 2030 and 30% by 2050 [5], [6].

In practice, system operators typically rely on experience and rule-based heuristics to schedule PSPS, such as the transmission line and area wildfire risk heuristics [7]. [7] shows that because both of these wildfire risk-based heuristics do not consider how network de-energizations affect optimal power flows in the network, more system wildfire risk is present for the same demand served on networks de-energized by field

heuristics than by using their optimal power shut-off (OPS) framework.

The OPS framework has been extended in several directions to include additional planning and investment decisions that would affect PSPS strategies [8]–[12]. [8] optimizes investments in distributed energy resource (DER) infrastructure (e.g. distributed solar and wind) and line hardening measures to reduce cumulative system wildfire risk and improve load delivery in regions of the RTS-GMLC and WECC more vulnerable to PSPS events. [9] incorporates $N-1$ security contingencies to robustify PSPS operation to unexpected line failures. [10] considers how de-energizations can disproportionately affect certain areas of the grid and suggests that operators should add fairness functions, such as the minimizing maximum load shed and minimizing a weighted penalized load shed, to PSPS planning to spread the burden of load shed and de-energizations across the grid.

However, the OPS defined in [7]–[11] does not consider commitment and operational costs and may choose more costly commitment and operational strategies. In OPS, developing appropriate weights for trading off normalized load loss versus normalized wildfire risk relies heavily on operator experience. Instead, we propose framing all objectives in terms of economic costs. Similar to the present work, [12] considers generator production costs in the deterministic objective function and monetizes line shut-offs; however, [12] does not consider any time-coupled constraints to model the scheduling limitations of generator dispatch and line de-energizations. [12] does not include ramping and commitment constraints, delays in restarting transmission lines after damages, and generator commitment costs.

Furthermore, the optimization models in [7]–[12] solve only the deterministic version of the PSPS by assuming perfect forecasts of both nodal demands and wildfire risk of grid components. [13] proposes a probabilistic DER planning model for PSPS events in Chile by minimizing the expected costs of investment, operation, and unserved energy. They note that there is large uncertainty in the sampled probability distribution of the outage scenarios used in the stochastic optimization. This uncertainty could drive away risk-averse investors because they may be more interested in viewing scenarios that generate worse-case profits rather than minimizing expected costs from a much larger selection of possible outage scenarios. [13] left studying the impacts of investor risk aversion to high planning and operating costs due to uncertain outage scenarios for future work. [14] constructs a robust unit commitment problem to model resilient operations during extreme weather events. [14] considers uncertainties in

Ryan Greenough, Kohei Murakami, Michael Davidson, and Adil Khurram are with the Department of Mechanical and Aerospace Engineering, University of California at San Diego, La Jolla, CA 92093 USA (e-mail: rgreenou@ucsd.edu; k1murakami@ucsd.edu; mrdavidson@ucsd.edu; akhurram@ucsd.edu)

Jan Kleissl is with the Center for Energy Research, Department of Mechanical and Aerospace Engineering, University of California at San Diego, La Jolla, CA 92093 USA (e-mail: jkleissl@ucsd.edu).

operational parameters and explores how wildfire spread can affect the thermal limits of transmission lines. However, [14] takes a risk-neutral approach to minimizing operational costs and does not consider how a risk-averse approach could alter line de-energizations and unit commitment decisions.

In this work, a mean-risk two-stage stochastic version of the PSPS (SPSPS) is formulated. A risk-averseness parameter β trades-off between minimizing the total expected costs with the CVaR $_{\epsilon}$ costs. Uncertainty is introduced in the maximal demand served for each bus in the network. The risk averseness parameter incorporates an operator's tendency to reduce spending when demand scenarios generate higher total economic costs (i.e. sum of the commitment and operational costs). Wildfire risk is represented by the Wildland Fire Potential Index (WFPI) and daily WFPI forecasts from the USGS are mapped to each transmission line. Our framework discourages operating transmission lines in fire-prone regions via a tolerance level set by the operator, R_{tol} . Real-time optimized device shut-offs and power injections are determined on a rolling horizon basis for the IEEE 14 bus transmission grid.

Our main contribution is modeling the non-anticipatory nature of preemptive commitment and line de-energizations performed during PSPS events and provide operators with the ability to be risk-averse to high economic costs. All prior work assumes operators are risk-neutral toward different cost scenarios. Several works assume operators can perfectly anticipate demands ([7]–[10], [12]) or instantaneously adjust generator commitment status ([7]–[12], [14]). To overcome this gap in the literature, we propose a two-stage stochastic day-ahead unit commitment model that incorporates uncertainties in demand forecasts and different timescales of operation while minimizing shut-down and start-up generation costs, operational costs, and the cost of unserved demand subject to a predefined level of risk for transmission line damages due to nearby wildfires.

Applying the model we are able to generate several novel findings and improved outcomes:

- 1) As opposed to deterministic strategies that are both popular in the literature, such as the OPS in [7]–[10] and widely used in the field, we include commitment and operational costs into the optimization, which reduces total expected costs.
- 2) We demonstrate that risk-averse operators can reduce the costs of operation in high-demand scenarios but at the possible expense of losing more demand at buses to blackouts.

The rest of the paper is organized as follows. Section II introduces the PSPS formulations. Section III details results for the deterministic and stochastic PSPS unit commitment in wildfire-prone regions on the IEEE 14-bus system. Section IV summarizes and concludes the paper.

II. MODELING PUBLIC SAFETY POWER SHUT-OFFS FOR WILDFIRE RISK MITIGATION

A two-stage problem is presented in which operators first make day-ahead decisions, such as generator commitments and transmission line de-energizations, then make real-time adjustments to supply and demand mismatches through operational

decisions, including load shedding and generation adjustments. Day-ahead decisions are influenced by day-ahead demand and wildfire risk forecasts and real-time decisions are influenced by realizations of real-time demand (see Figure 1).

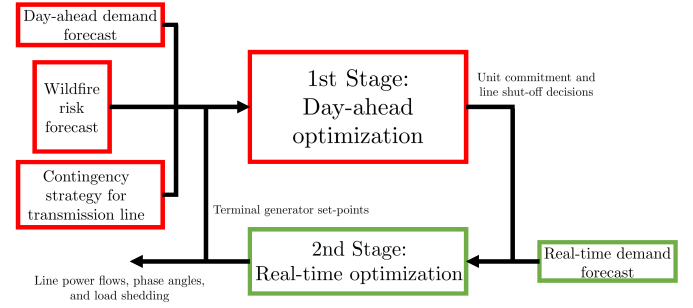


Fig. 1: Block diagram showing the data inputs and decision outputs for each stage of the two-stage stochastic optimization.

A. Preliminaries

Let $\mathcal{P} = (\mathcal{B}, \mathcal{L})$ be the graph describing the power grid where $\mathcal{B} = \{1, \dots, B\}$ is the set of B buses in the network, and \mathcal{L} is the set of edges such that two buses $i, j \in \mathcal{B}$ are connected by a transmission line if $(i, j) \in \mathcal{L}$. The set of buses with generators and loads are collected in \mathcal{G} and \mathcal{D} respectively, and $\mathcal{H} = \{1, \dots, H\}$ is the set of time indices over the horizon H of the optimization problem. A DC-OPF is used to approximate the line power flows and bus power injections; all references to power are to its active power. At any timestep t , the power injected by the generator at bus $g \in \mathcal{G}$ is denoted by $p_{g,t}$. Similarly, $p_{d,t}$ is the load at bus $d \in \mathcal{D}$. Power flowing through the line $(i, j) \in \mathcal{L}$ is $p_{ij,t}$ and the phase angle at bus $i \in \mathcal{B}$ is denoted by $\theta_{i,t}$. Finally, the binary variables are denoted by $z \in \{0, 1\}$ with an appropriate subscript to capture component shut-off decisions.

B. Objective Function

The objective of the stochastic PSPS with unit commitment is to minimize the cost of starting and shutting off generators (f^{uc}), operating costs (f^{oc}) of generators, and the cost associated with the fraction of load shed (f^{VoLL}), called the value of lost load (VoLL) defined as

$$f^{\text{uc}}(z_g^{\text{up}}, z_g^{\text{dn}}) = \sum_{t \in \mathcal{H}} \left(\sum_{g \in \mathcal{G}} C_g^{\text{up}} z_{g,t}^{\text{up}} + C_g^{\text{dn}} z_{g,t}^{\text{dn}} \right), \quad (1)$$

$$f^{\text{oc}}(\mathbf{p}_g) = \sum_{t \in \mathcal{H}} \left(\sum_{g \in \mathcal{G}} C_g p_{g,t} \right), \quad (2)$$

$$f_{\xi}^{\text{VoLL}}(\mathbf{x}_d, \mathbf{p}_d, \xi) = \sum_{t \in \mathcal{H}} \left(\sum_{d \in \mathcal{D}} C_d^{\text{VoLL}} (1 - x_{d,t}) p_{d,t,\xi} \right), \quad (3)$$

where C_g^{up} and C_g^{dn} are the generator start up and shut down cost which together with the binary variables $z_{g,t}^{\text{up}}$ and $z_{g,t}^{\text{dn}}$

capture the one-time cost incurred when bringing a generator online or offline. C_g is each generator's associated marginal cost. Only demand uncertainty is considered which is captured in ξ and the corresponding demand is given by $p_{d,t,\xi}$. The fraction of the load served is $x_{d,t} \in [0, 1]$ and C_d^{VoLL} is the cost incurred as a result of shedding $(1 - x_{d,t})$ proportion of the load, $p_{d,t,\xi}$. Let $p_g = (p_{g,1}, \dots, p_{g,H})^\top$ be the vector of $p_{g,t}$ for generator g , then p_g for all generators are denoted as $\mathbf{p}_g = (p_1, \dots, p_G)^\top$. The variables $\mathbf{p}_{d,\xi}$, \mathbf{x}_d , \mathbf{z}_g^{up} , \mathbf{z}_g^{dn} are defined in a similar manner. The resulting objective function is given by,

$$\Pi_\xi = f^{\text{uc}}(\mathbf{z}_g^{\text{up}}, \mathbf{z}_g^{\text{dn}}) + f^{\text{oc}}(\mathbf{p}_g) + f_\xi^{\text{VoLL}}(\mathbf{x}_d, \mathbf{p}_{d,\xi}) + R_{\text{slack}}, \quad (4)$$

where R_{slack} is a design parameter, defined in Section III-E, and is added to prioritize low-risk line shut-off strategies. Due to the uncertainty ξ , the objective function is stochastic, therefore, the risk-neutral PSPS aims to minimize the expected value of Π_ξ . A scenario-based two-stage approach is used to solve the resulting stochastic optimization problem as described in Section III-F.

C. Unit Commitment Constraints

The unit commitment constraints (5a)-(5b) are used to enforce minimum up time (t_g^{MinUp}) and down time (t_g^{MinDn}) of generators. Similarly, the constraint (5c) guarantees consistency between the binary variables $z_{g,t}^{\text{up}}$ and $z_{g,t}^{\text{dn}}$. In all simulations, it is assumed that all generators are initially off.

$$z_{g,t} \geq \sum_{t' \geq t - t_g^{\text{MinUp}}} z_{g,t'}^{\text{up}}, \quad \forall g \in \mathcal{G}, t \in \mathcal{H} \quad (5a)$$

$$1 - z_{g,t} \geq \sum_{t' \geq t - t_g^{\text{MinDn}}} z_{g,t'}^{\text{dn}}, \quad \forall g \in \mathcal{G}, t \in \mathcal{H} \quad (5b)$$

$$z_{g,t+1} - z_{g,t} = z_{g,t+1}^{\text{up}} - z_{g,t+1}^{\text{dn}}, \quad \forall g \in \mathcal{G}, t \in \mathcal{H} \quad (5c)$$

D. Operational Constraints

The power of generator g is limited as

$$z_{g,t} \underline{p}_g \leq p_{g,t} \leq z_{g,t} \bar{p}_g, \quad \forall t \in \mathcal{H}, g \in \mathcal{G}, \quad (6)$$

where \underline{p}_g and \bar{p}_g are the minimum and maximum power generation limits of generator g .

The auxiliary variable $p_{g,t}^{\text{aux}}$ is introduced in (7a) as equal to the difference in generation of generator g from its minimum output limit (\underline{U}_g) and zero otherwise. The constraint (7b) prevents ramp violations during the startup process.

$$p_{g,t}^{\text{aux}} = p_{g,t} - \underline{p}_g z_{g,t}, \quad \forall g \in \mathcal{G}, t \in \mathcal{H}, \quad (7a)$$

$$\underline{U}_g \leq p_{g,t+1}^{\text{aux}} - p_{g,t}^{\text{aux}} \leq \bar{U}_g \quad \forall g \in \mathcal{G}, t \in \mathcal{H}. \quad (7b)$$

It is assumed that when a line is switched off, it remains off for the remainder of the day which is enforced by,

$$z_{ij,t} \geq z_{ij,t+1} \quad \forall (i, j) \in \mathcal{L}, t \in \mathcal{H}. \quad (8)$$

To model power flow through the transmission lines, the DC-OPF approximation is used as

$$p_{ij,t} \leq -B_{ij} (\theta_{i,t} - \theta_{j,t} + \bar{\theta} (1 - z_{ij,t})). \quad (9a)$$

$$p_{ij,t} \geq -B_{ij} (\theta_{i,t} - \theta_{j,t} + \underline{\theta} (1 - z_{ij,t})), \quad (9b)$$

$$\underline{p}_{ij,t} z_{ij,t} \leq p_{ij,t} \leq \bar{p}_{ij,t} z_{ij,t} \quad (9c)$$

for all $t \in \mathcal{H}$ (i, j) $\in \mathcal{L}$. Constraints (9a) and (9b) limit power flow $p_{ij,t}$ between maximum and minimum limits, where B_{ij} is the susceptance of the line. When $z_{ij,t} = 1$, (9a) and (9b) hold with equality. When $z_{ij,t} = 0$, the power flow across transmission line (i, j) at time t is zero and the phase angle $\theta_{i,t}$ is limited between its maximum ($\bar{\theta}$) and minimum ($\underline{\theta}$) limits. Constraint (9c) enforces the thermal limits, $\underline{p}_{ij,t}$ and $\bar{p}_{ij,t}$, on power flow, $p_{ij,t}$. The decision variable, $z_{ij,t}$, is used in constraint (9c) to ensure that if $p_{ij,t} = 0$ the line from bus i to j is de-energized. Finally, the bus power balance at each $t \in \mathcal{H}$ and every bus $i \in \mathcal{B}$ is given by the following equality constraint,

$$\sum_{g \in \mathcal{G}_i} p_{g,t} + \sum_{(i,j) \in \mathcal{L}} p_{ij,t} - \sum_{d \in \mathcal{D}_i} x_{d,t} p_{d,t,\xi} = 0. \quad (10)$$

E. Constraint for de-energizing no less than k lines

During the day ahead planning phase, the grid operator has the flexibility to control the maximum number of active lines based on WFPI risk tolerance. Constraint (11) represents a line shut-off strategy that constrains the total number of active lines so that the total line risk does not exceed R_{tol} which is an operator-driven parameter (measured in WFPI [15]). R_{tol} guarantees a certain level of security for the system while also penalizing the operation of transmission lines within regions of higher WFPI

$$\sum_{(i,j) \in \mathcal{L}} z_{ij,t} R_{ij,t} \leq R_{\text{tol}}, \quad \forall t \in \mathcal{H}. \quad (11)$$

Constraint (12) is similar to the standard $N-k$ shut-off strategy in which the operator defines the maximum number of lines that are active in the system for the complete time horizon without considering the wildfire risk [16].

$$\sum_{(i,j) \in \mathcal{L}} z_{ij,t} \leq |\mathcal{L}| - |\mathcal{K}|, \quad \forall t \in \mathcal{H} \quad (12)$$

Operators use (11) or (12) to obtain a line shut-off strategy that achieves a lower risk. However, in the case of (11), there are multiple solutions with the same number of active lines but with different wild fire risk that still satisfy (11). To prioritize a low-risk solution, (11) is modified to an equality constraint with a slack variable R_{slack} that minimizes the difference from the minimum wildfire risk for a given number of active lines as

$$\sum_{(i,j) \in \mathcal{L}} z_{ij,t} R_{ij,t} - R_{\text{slack}} = R_{\text{tol}}, \quad \forall t \in \mathcal{H}, \quad (13a)$$

$$0 \leq R_{\text{slack}} \leq \bar{R}_{\text{slack}}, \quad (13b)$$

where \bar{R}_{slack} is a design parameter chosen to upper bound violation.

F. Two Stage Stochastic Problem

A two-stage scenario-based formulation is developed in this section to include demand uncertainty. Unit commitments (z_g^{up} ,

z_g^{dn}, z_g and transmission line shut-offs (z_{ij}) are determined for the entire optimization horizon and thus modeled as first-stage decisions. The scenarios are drawn from the historical real data by using a scenario reduction technique which selects a set of K demand scenarios, $\omega \in \Omega = \{\omega_1, \dots, \omega_K\}$. The real-time generator output ($p_{g,\omega}$) and load served ($x_{d,\omega}$) are determined in the second stage depending on the realized demand ($p_{d,\omega}$).

1) *First Stage Formulation*: The objective function for the first stage considers the conditional value at risk (CVaR $_\epsilon$) and is given by,

$$\min (1 - \beta) \mathbb{E}[\Pi_\omega] + \beta \text{CVaR}_\epsilon(\Pi_\omega) \quad (14)$$

s.t.

$$\Pi_\omega = f^{\text{uc}}(z_g^{\text{up}}, z_g^{\text{dn}}) + f^{\text{oc}}(p_{g,\omega}) + f^{\text{VoLL}}(x_{d,\omega}, p_{d,\omega}) + R_{\text{slack}}, \quad (15)$$

Line Contingencies: {(11), (13a)&(13b), or (12)} and (8)

Unit Commitment Constraints: (5a) – (5c)

Generator Capacity Bounds: (6)

Generator Ramping Constraints: (7a) – (7b)

Optimal Power Flow Constraints: (9a) – (9c)

Day-ahead Demand Balance Constraints: (10)

CVaR Constraints: (18a) – (18c)

$$\forall t \in \mathcal{H}, i \in \mathcal{B}, \forall \omega \in \Omega$$

In (14), the outer weighted sum with weighting parameter β is the balance between the expected value of the total costs for each scenario (denoted Π_ω) among all scenarios $\omega \in \Omega$, and its ϵ -quantile expected shortfall or CVaR $_\epsilon(\Pi_\omega)$. To reduce the computational complexity of taking the expectation over all possible demand scenarios, a tree scenario reduction algorithm, developed in [17], is used to reduce the number of demand scenarios to a smaller finite set of demand scenarios Ω from the day-ahead forecast. The probability of occurrence of a given scenario $\omega \in \Omega$ is denoted by π_ω . The expectation is then taken over the set of reduced scenarios,

$$\mathbb{E}[\Pi_\omega] = \sum_{\omega \in \Omega} \pi_\omega \Pi_\omega. \quad (16)$$

The standard risk-neutral two-stage unit commitment problem optimizes for expected total costs [18]. Wildfires are less frequent high-impact events and call for non-routine operations. A risk-averse decision-making strategy, rather than a purely risk-neutral one, is used to handle the effect of variability in the demand. A natural approach to handling volatility in the costs is a mean-variance approach (e.g. Markowitz approach). However, mean-variance optimization penalizes upper-tail and lower-tail costs equally. Instead, a widely adopted convex and coherent risk metric, conditional value at risk, is used to penalize upper-tail costs [18]–[20]. For a discrete probability distribution, CVaR $_\epsilon$ of Π_ω is mathematically defined as,

$$\text{CVaR}_\epsilon(\Pi_\omega) = \min_{\nu} \left\{ \nu + \frac{1}{1 - \epsilon} \mathbb{E}[\max\{\Pi_\omega - \nu, 0\}] \right\} \quad (17)$$

At optimality, the auxiliary variable, ν , is commonly referred to as the value at risk (VaR) or minimum cost at an ϵ -

confidence level. The CVaR $_\epsilon(\Pi_\omega)$ can be approximated as a linear program with $\gamma_\omega := \max\{\Pi_\omega(\cdot, \xi_\omega) - \nu, 0\}$, ν as an auxiliary variable, and $\epsilon \in [0, 1]$.

$$\nu + \frac{1}{1 - \epsilon} \sum_{\omega \in \Omega} \pi_\omega \gamma_\omega = \text{CVaR}_\epsilon(\Pi_\omega) \quad \forall \omega \in \Omega \quad (18a)$$

$$\Pi_\omega - \nu \leq \gamma_\omega \quad \forall \omega \in \Omega \quad (18b)$$

$$0 \leq \gamma_\omega \quad \forall \omega \in \Omega \quad (18c)$$

Two parameters contribute to the operator's level of risk-averseness: ϵ and β . By definition, ϵ adjusts the operator's averseness to high-tail economic costs. The economic costs in each scenario are strongly influenced by the amount of demand served in each scenario due to the high value assigned to the Value of Lost Load. When $\epsilon = 0$, CVaR $_\epsilon(\Pi_\omega) = \mathbb{E}(\Pi_\omega)$ and the operator is risk-neutral. When $\epsilon = 1$, CVaR $_\epsilon(\Pi_\omega) = \sup\{\Pi_\omega\}$ and the operator is the most-risk averse. The confidence level, ϵ , is fixed at 95%. For normally distributed cost scenarios, 95% is a commonly used baseline confidence level equivalent to considering scenarios over 1.96 standard deviations from the mean. By construction increasing β (for a fixed ϵ) gives more penalty to the more risk-averse term in the objective CVaR $_\epsilon$ and increases the mean-CVaR $_\epsilon$ objective. Due to the shifting of weight from mean to CVaR $_\epsilon$, increasing β (for a fixed ϵ) increases the mean costs and decreases the CVaR $_\epsilon$ costs in the mean-CVaR $_\epsilon$ objective.

2) *Second Stage Formulation*: After the generator commitments and transmission line shut-off decisions are made, in real-time the system operator must decide on the power consumption at each hourly interval in real-time. The second stage is implemented in a receding horizon fashion [21]. Instead of optimizing costs over demand scenarios / forecasts $\omega \in \Omega$, realized samples of demand, $p_{d,\omega'}$, are used from a set of real-time samples Ω^{RT} . One realization of demand is used in the analysis in Section III-C. The deterministic PSPS formulation is a special case of the stochastic PSPS problem in which it is assumed that the uncertainty is captured in a single scenario that represents the expected demand (i.e. $\mathbb{E}[p_{d,\xi}]$).

III. RESULTS

In this Section, the differences in optimal decisions and costs for the deterministic and stochastic PSPS frameworks are analyzed for day-ahead unit commitment on the IEEE 14-bus system.

A. Data and Test Case Description

WFPI has been used in recent research works, e.g. [7]–[10], to assess the risk of damage to power system components from nearby wildfires. WFPI describes the ratio of live to dead fuel and includes modifiers for wind speed, dry bulb temperature, and rainfall [15]. The USGS generates WFPI forecasts for the continental US up to seven days in the future. An assignment of WFPI values to the IEEE 14 bus network is depicted in Figure 2.

The grid model used for analysis is the modified IEEE 14 bus system as shown Fig. 2, consisting of 2 generators (at buses 1 and 2), 11 loads (one load each at buses 2-6 and 9-14), and 20 transmission lines. The buses are assumed to be

located at 14 locations in Southern Nevada and Northwestern Arizona that typically experience large wildfire risk throughout the year. Generator costs, power, and energy capacities are provided in Table I. Hourly load profiles are obtained from [22]. The load profile for each of the 14 buses is then obtained by scaling the profile so that the maximum load is equal to the load defined in [23].

From the USGS fire data products page [15], day-ahead forecasts are downloaded in .tiff format and combined to form timeseries of WFPI predictions for each of the 14 locations. Each .tiff file contains a mesh in which each point is associated with a WFPI value and a pixel with (x, y) coordinates. The four nearest neighbors from the .tiff grid mesh are averaged to form the WFPI forecast of the bus location. Forecasts for lines on the IEEE 14-bus are assumed to be the maximum WFPI value experienced on the straight line between connecting buses. In this way, bus WFPI forecasts provide a conservative estimate of the transmission line WFPIs.

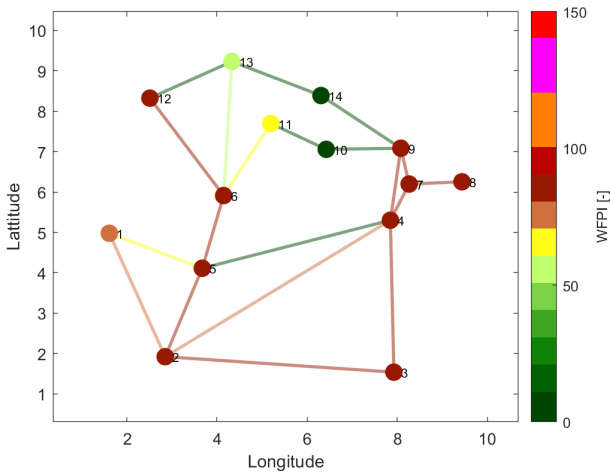


Fig. 2: An IEEE 14-bus system schematic with each transmission line and bus color-coded to depict its wildfire risk value. Note the arbitrary layout of the buses comes from [23]; the distances between buses are not to scale WFPI values were recorded on October 11th, 2015 in the southwestern U.S. [15].

TABLE I: IEEE 14-bus system generator statistics [22], [23]

	$\bar{p}_g, \underline{p}_g$ (MW)	$\bar{U}_g, \underline{U}_g$ (MW/h)	$t_g^{\text{MinUp}}, t_g^{\text{MinDn}}$ (h)
Gen 1	340, 0	± 248.4	8.0, 4.0
Gen 2	59, 0	± 22.0	2.0, 2.0
	C_g (\$/MWh)	$C_g^{\text{up}}, C_g^{\text{dn}}$ (\$)	
Gen 1	7.92	280, 280	
Gen 2	23.27	56, 56	

To implement the two-stage stochastic PSPS, demand scenarios are generated via a tree reduction algorithm from [17]. The optimization horizon of interest is one day. The tree scenario reduction method analyzes three months of prior demand forecasts for the total cumulative load for the region

TABLE II: Optimization approaches

Name	Objective function	Risk constraint
NMKS	$f_{uc} + f_{VoLL} + f_{oc}$	$\sum_{(i,j) \in \mathcal{L}} z_{ij,t} \leq \mathcal{L} - \mathcal{K} $
MNWF	$f_{uc} + f_{VoLL} + f_{oc}$	Heuristic: activate k lines w/ k lowest $R_{ij,t}$ values
WFNC	f_{VoLL}	$\sum_{(i,j)} z_{ij,t} R_{ij,t} \leq R_{tol}$
WFPI	$f_{uc} + f_{VoLL} + f_{oc}$	$\sum_{(i,j)} z_{ij,t} R_{ij,t} \leq R_{tol}$
WFSL	$f_{uc} + f_{VoLL} + f_{oc}$	$\sum_{(i,j)} z_{ij,t} R_{ij,t} - R_{slack} = R_{tol},$ $0 \leq R_{slack} \leq \bar{R}_{slack}$

in which the 14 IEEE buses reside. The output is a scenario tree of 5 representative demand scenarios for the next day. The five demand scenarios are max-scaled and proportionally mapped to each of the static loads given in the IEEE 14-bus system datasheet. To adjust the scenario set to include less probable high-demand scenarios, at each time step a normal distribution is fit to the five demand scenarios. At each time step, $t \in \mathcal{H}$, there are five new samples: the sample mean, sample mean ± 1 standard deviation, and sample mean ± 2 standard deviations for that given time step. The five new scenarios include timeseries of all sample mean, all sample means ± 1 standard deviation, and sample mean ± 2 standard deviations. The five newly generated scenarios are shown in Figure 3. The stochastic optimization problem is converted to a deterministic problem with one power balance constraint for each demand scenario (10).

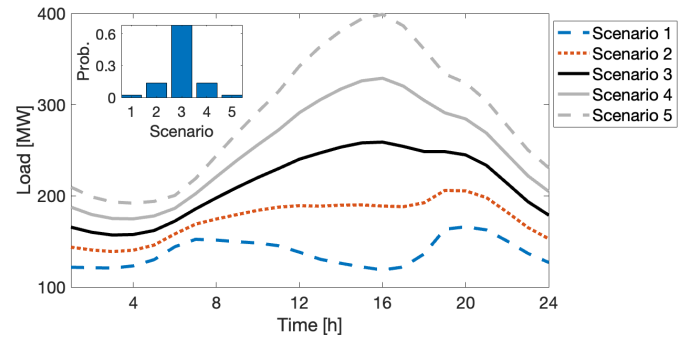


Fig. 3: Load scenarios (mean, ± 1 std. dev. and ± 2 std. dev.) for the IEEE 14-bus system derived from the tree reduction load profiles for the RTS-GMLC for October 11, 2020. The probabilities of occurrence of each demand scenario are shown in the insert in the upper left corner.

B. Comparison of different line outage strategies

Five deterministic line outage strategies are shown in Table II. For simplification, only the load at the moment of peak expected demand, hour 16 in Figure 3, is considered. [7]–[12] did not study generator commitment. Generator commitment statuses are analyzed in this paper because the selection of active generators highly influences total production costs. In $N-k$ (NMKS), $|\mathcal{K}|$ lines are de-energized so that the total cost is minimized. Its drawback is that its optimization model

is not aware of wildfire risk. The Minimum WFPI heuristic (MNWF) is the transmission heuristic approach described in [7] and is commonly used in practice by system operators. Weighted WFPI with No Commitment or Operating Costs (WFNC) is a reformulation of the approach proposed in [7]–[10] in which total load served and wildfire risk are considered. The difference between WFNC and [7]–[10] is that allowable wildfire risk (R_{tol}) is treated as a constraint rather than an objective so as to keep all terms in the objective function in terms of financial costs. The weighted-WFPI approach (WFPI) has the same risk constraint as WFNC except that it considers commitment and operating costs in addition to VoLL. In Weighted-WFPI approach with Slack (WFSL), the WFPI approach is modified to include constraint (13b) that ensures the transmission line topology also optimizes wildfire risk rather than just selecting a feasible transmission line topology, which is a drawback of the WFPI approach.

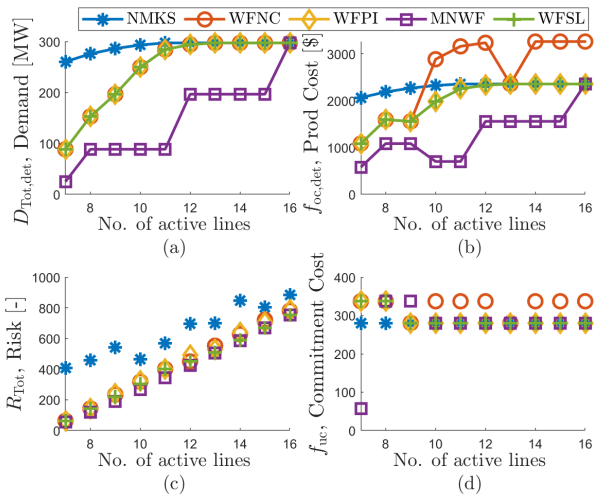


Fig. 4: Effect of the number of active lines on a) demand, b) production costs, c) wildfire risk, and d) commitment costs for the five benchmark optimization approaches described in Table II at the moment of peak demand (hour 16 of the day).

Simulation results for all approaches are shown in Figure 4. For NMKS, $|\mathcal{K}|$ is swept from 0 to 20 active lines stepping one active line. For the other approaches, R_{tol} is swept from 0 to the sum of all 20 WFPI line values: 1,089. R_{tol} is the set of minimum WFPI for a given number of active lines. Since 6 lines in the network have zero WFPI, all approaches except NMKS reach the same solution for active line settings of 6 lines or less; that solution is to produce 26 MW at bus 2 using Gen 2.

Due to the flexibility present in the IEEE 14-bus system, only 11 active lines are needed for NMKS to satisfy all of the demand and achieve the minimum cost of serving the maximum amount of demand (Figure 4(a)). However, NMKS achieves this solution at the cost of higher wildfire risk than other approaches. 13 active lines are needed for approaches WFNC, WFPI, and WFSL to serve all demand. With less than 13 active lines, total demand increases as the number of active lines increases.

The network structure greatly affects the production costs. While MNWF achieves the lowest production cost at each active line setting, it does this at the cost of producing the most load-shed compared to other approaches. And it is not until 16 lines are active that all of the demand is served. Additionally, MNWF cannot dispatch Gen 1 until at least 8 lines are active. This is because Gen 1 is located at bus 1 and the lines connected to bus 1 (Line 1-5 and Line 1-2) are the lines with the 8th and 10th smallest WFPI values in the network as shown in Fig. 2. MNWF needs at least 11 lines to be active before the heuristic decides to exclusively use the least costly generator (Fig. 4(d)).

In WFNC, WFPI, and WFSL both generators need to be committed when there are 7 and 8 active lines because the resulting network is divided into two disjoint networks. Given the relative sizing and location of the less costly generator Gen 1, this generator is committed for active line settings 8-20 for all approaches. When more than 9 lines are active, only the less costly generator, Gen 1, needs to be dispatched for NMKS, WFPI, and WFSL as shown in Figure 4(d); the commitment cost for those cases, \$280, is equal to the start-up cost of Gen 1.

All Approaches achieve monotonic increases in demand with increases in active lines. NMKS has a monotonic increase in costs with an increase in active lines. WFPI and WFSL have similar trends in production costs versus active lines: increases in production costs from 6-8 active lines, a drop in costs with 9 active lines, then followed by a monotonic increase in production costs for 10 or more active lines (Fig. 4(b)). A drawback of not including production costs in WFNC is that there can be solutions that are more expensive yet meet the same demand with the same number of active lines. For example, in Fig. 4(b) the production costs of WFNC relative to NMKS, WFPI, and WFSL increase for active line setting of 10-12, 14-16 lines. In WFNC, the dispatch of the more costly second generator leads to production cost increases between roughly 39-46% (or \$905 in those cases of 10-12, 14-16 active lines).

By constraining the number of active lines to the lowest amount of wildfire risk per line, MNWF displays the lowest possible wildfire risk; however, it reduces the load served for less than 16 active lines. Since wildfire risk is not included in the objective function, NMKS, WFNC, and WFPI are not guaranteed to generate active line strategies with the lowest wildfire risk for the same economic cost. There may be multiple line de-energization strategies that generate the same economic cost and are within the wildfire risk tolerance. For instance, given an R_{tol} of 266.2, WFNC, WFPI, and WFSL serve 196.6 MWh at a cost of \$1,557.4 with 9 lines; 8 of those are in common (totaling a WFPI of 143.5). WFNC activates line 2-4 (77.1 WFPI), WFPI 2-5 (83.2 WFPI), and WFSL 1-5 (63.1 WFPI). NMKS improves load delivery by 45% (or 286.3 MWh). However, it only activates 2 of the 6 zero WFPI lines (9-10 and 13-14) and increases wildfire risk by 145% (541 WFPI). Approach WFSL generates lower wildfire risk as compared to NMKS. And WFSL generates lower wildfire risk than WFNC and WFPI despite serving the same amount of demand. This is accomplished by the slack variable that

minimizes the difference from the minimum wildfire risk (R_{tol}) for a given number of active lines as described in Section II-E. Another drawback to WFNC and WFPI is that finer sweeps of R_{tol} may be needed to understand the relationship between R_{tol} and the optimized number of active lines (a discrete variable). For instance, if the operator chooses an R_{tol} of 56.89, MNWF activates the six zero risk lines and line 6-13 (the line with the lowest non-zero risk of a line). The addition of 6-13 does not improve the load delivery when both generators are isolated from the rest of the network. As a result of this zero benefit to the load delivery, WFNC and WFPI choose to only activate the six lines with zero WFPI until the WFPI tolerance is at least 63.10. WFSL increases total system line risk to WFPI 63.10 to add line 1-5 instead of 6-13. While the system wildfire risk is increased by 10.9%, load delivery is increased by 255% (from 24.9 MW to 88.49 MW), which justifies the commitment of Gen 1.

Overall Figure 4 indicates that WFSL is the best approach of the five for deterministic PSPS. WFSL minimizes commitment, production, and VoLL costs and tightens the bounds of wildfire risk tolerance. The presence of the slack variable in WFSL allows operators to still use simple heuristics to step through wildfire risk tolerance levels. WFSL does not require a finer sweep of risk tolerances (as needed in WFNC or WFPI) to outperform an $N-k$ approach strategy in wildfire mitigation.

C. Stochastic PSPS (SPSPS) results

In the simulations, ϵ is fixed at the 95% confidence level and the value of lost load is set to 1,000 \$/MWh [14], [24], [25]. Since the value of losing 1 MWh is at least one order magnitude higher than the cost to produce 1 MWh, the VoLL is typically the largest contributor to the total economic costs. For simulations, the step size of β is taken as 0.1; all samples are summarized by $\beta \in \{0, 0.1, 0.2, 0.3, \dots, 0.9, 1\}$.

1) *Sweep of risk aversion levels for first stage:* To highlight the cost differences between the risk-neutral and risk-averse operating strategies, the case when the operator selects 12 active lines is considered.

The risk-neutral strategies correspond to $\beta \in [0, 0.1]$ and $\beta \in [0.2, 1]$ leads to the risk-averse strategies. Optimal expected and CVaR total costs, production costs, total demand served, and generator commitments are given in Table III. It should be emphasized that only the first-stage generator commitment and line de-energization decisions are used in the second stage while the generator powers and load shed are discarded and re-optimized for a particular realization of demand in the second stage.

Figure 5 summarizes differences in the generation, lost load, generating costs, and VoLL costs that arise between risk-neutral ($\beta \in [0, 0.1]$) and risk-averse ($\beta \in [0.2, 1]$) decisions. Note that the solutions for $\beta = 0.8$ and $\beta = 0$ are the ones plotted but any β within the respective risk-averse or risk-neutral ranges results in the same first-stage generator commitments, line de-energizations, and second-stage decisions.

In the case of 12 active lines, the risk-neutral decision maker commits the less costly Gen 1 until it becomes cost-effective

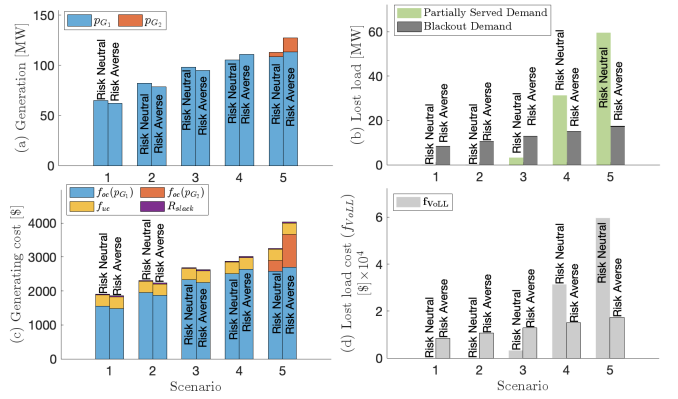


Fig. 5: SPSPS (a) generation, (b) load shedding, (c) total costs (excluding VoLL), and (d) VoLL costs for the IEEE 14-bus system optimized at the moment of peak demand (hour 16). Left bars are risk-neutral results for $\beta = 0$ and right bars are risk-averse results for $\beta = 0.8$. Subplots (a)-(d) together show that for the risk-averse strategy, higher production costs in scenarios 4 and 5 are overcome by savings in VoLL.

to commit Gen 2 in the highest-demand scenario. The peak demand is equal to the maximum combined capacity of the two generators; however, transmission line power flow limits lead to unserved energy in the three higher demand scenarios. In the highest demand scenario, lines 2-5 and 2-3 reach their power flow limits. The risk-neutral approach not only uses less of Gen 1's capacity but also less combined generator capacity in the highest demand scenario than the risk-averse approach (see Fig. 5(a) for comparison of generation and Table IV for differences in transmission line de-energization). VoLL costs are purely a function of the risk-neutral decisions maxing out power flow line limits during the three highest demand scenarios (see Figs. 5(b) and 5(d)).

The risk-averse objective of minimizing CVaR total economic costs is accomplished by minimizing a weighted average of costs among the top 5% of scenario costs. Given the distribution of costs in Fig. 3, the weighted average is 54.4% of the total cost of the fourth scenario and 45.6% of the total cost of the fifth scenario. As seen in Figure 5(c), this weighted average of costs in the fourth and fifth scenarios is less for the risk-averse decisions than it is for the risk-neutral decisions. In the 12 active lines setting, the risk-averse approach is accomplished by altering the network configuration (see Table IV) to achieve lower conditional expected total costs among the two highest demand scenarios. Power flows are not exceeded in any of the lines in the four lower demand scenarios, but the alteration of the network blackouts bus 6 for all scenarios. There is a small amount of 1.16 MW loss in the load at bus 3, p_{D_3} , (0.8% of 145 MW load) in the highest demand scenario for the risk-averse decisions. Therefore, the VoLL in each scenario for the risk-averse decision maker is mostly due to the blackout at bus 6. This effect is also observed in the Section III-C2 which considers the full 24-hour horizon. Specifically, the risk-averse operators reduce the expected costs of operation among the high-demand scenarios at the expense of losing more demand buses to blackouts.

TABLE III: SPSPS commitment and operational decisions and costs for the IEEE 14-bus system optimized at the moment of peak demand (hour 16). β is stepped every 0.1 from $\beta = 0$ (risk neutral) to $\beta = 1$ (most risk-averse). CVaR is calculated using equation (7) from [26].

Risk Aversion	Line Risk	Exp. Demand [MW]	CVaR _{0.95} Demand [MW]	Exp. Prod. Cost [\$]	CVaR _{0.95} Prod. Cost [\$]	Gen Commits	Exp. Cost [\$]	CVaR _{0.95} Cost [\$]	Highest Demand Cost [\$]
$\beta = 1$	464.3	281.8	355.2	2,243.7	3,104.0	2	18,106	19,551	21,408
$\beta \in [0.2, 0.9]$	464.3	284.4	355.2	2,267.5	3,104.0	2	15,463	19,551	21,408
$\beta \in [0, 0.1]$	450.0	289.4	327.1	2,297.4	2,684.3	2	10,472	47,213	62,824
Deter.	450.0	294.0	-	2,329.0	-	1	5,863	-	65,931

Table III shows that the risk-averse decision to blackout bus 6 leads to less expected production costs; however, the blackout of bus 6 in each load scenario increases expected total costs through higher expected VoLL costs. In the 12 active line setting, the risk-averse decisions lead to more CVaR_{0.95} production costs than risk-neutral decisions. However, the increase in CVaR production costs is due to serving a greater portion of the load; less lost load equates to less lost load costs and less total cost in the two high-demand scenarios.

The instance when the number of active lines equals 12 is a notable case because the most risk-averse ($\beta = 1$), risk-averse ($\beta \in [0.2, 0.9]$), risk-neutral ($\beta \in [0, 0.1]$), and deterministic approaches produce different total expected costs based on the level of risk aversion. The network for the deterministic case is depicted in Figure 6 to give the reader a baseline for comparison to strategies developed by the two-stage stochastic solution at different risk averseness levels.

Figure 6 and Table IV summarize the differences in transmission line de-energizations and expected demand served at various buses. At the bus level, compared to the deterministic case, there is a reduction in the expected demand at buses 4, 9, 10, and 13 for β from 0 to 0.1 (more risk neutral). This reduction in expected demand is due to power flow limits on line 5-6 restricting service to buses downstream of bus 6 in the higher demand scenarios of the risk-neutral optimization.

Then going from $\beta \in [0, 0.1]$ to $\beta \in [0.2, 1]$ (increasing in risk-averse level), there is a restoration of the demand at buses 4, 9, 10, and the lines 1-5, 2-4, 4-7, and 7-9. But there is a blackout at bus 6 and shut-offs of lines 2-5, 5-6, 6-11, and 6-13. As mentioned previously, this new configuration allows more of the capacity in Gen 1 and Gen 2 to be used. Finally, in the case when $\beta = 1$ (most risk-averse case), there is an additional reduction in the expected demand at bus 4 since only the CVaR_{0.95} term is considered in the optimization problem. The CVaR_{0.95} term optimizes costs in the two most costly demand scenarios (e.g. the fourth and fifth demand scenarios). Additional load loss in the three less costly lower demand scenarios occurs because those cost scenarios are not optimized.

Table III follows the anticipated trend that increasing β increases mean total costs and decreases CVaR_{0.95} total costs (explained in the last paragraph in Section II-F.1). The expected costs for the risk-averse strategies ($\beta \in [0.2, 0.9]$ and $\beta = 1$) are nearly \$5,000 and \$7,700 higher than the risk-neutral approach. On the other hand, CVaR_{0.95} costs for those

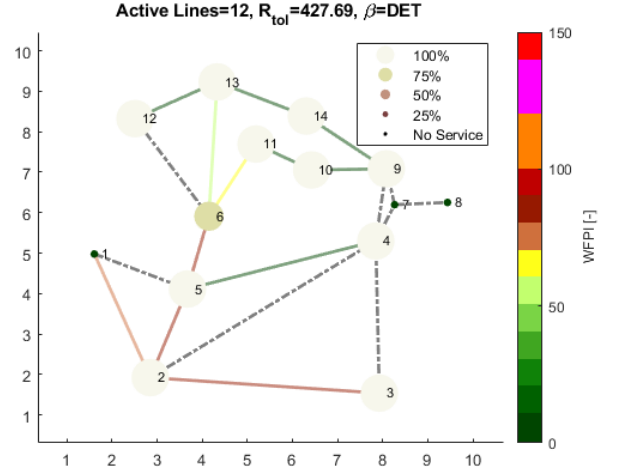


Fig. 6: Optimized deterministic 12-line shut-off strategies and load delivery to minimize commitment, production costs, and VoLL at the moment of peak demand. The size and color of buses indicate the fraction of the load being served. Black dashed lines indicate line de-energizations and black dot buses indicate no demand served.

TABLE IV: Differences between stochastic line de-energizations (z_{ij}^β) and the deterministic line de-energization (z_{ij}^{DET}). Differences between expected load served, $\mathbb{E}[p_{d,\omega}^\beta]$, and deterministic load served, $p_d^{\text{DET}}(\mathbb{E}[\xi])$. Ranges of risk averseness are $\beta \in [0, 0.1]$ and $\beta \in [0.2, 1]$. The increase in risk averseness levels leads to blackouts at Bus 6 and decreases in expected demand

β	$z_{ij}^\beta = 1, z_{ij}^{\text{DET}} = 0$	$z_{ij}^\beta = 0, z_{ij}^{\text{DET}} = 1$	
0.2 – 1	$z_{\{15,24,47,79\}}$	$z_{\{25,56,611,613\}}$	
0 – 0.1	-	-	
β	$\mathbb{E}[p_{d,\omega}^\beta] > p_d^{\text{DET}}(\mathbb{E}[\xi])$	$\mathbb{E}[p_{d,\omega}^\beta] < p_d^{\text{DET}}(\mathbb{E}[\xi])$	Blackout demand
1	-	PD_4	PD_6
0.2 – 0.9	-	-	PD_6
0 – 0.1	PD_6	$PD_{\{4,9,10,13\}}$	-

more risk-averse approaches are roughly \$27,500 less than the risk-neutral approach. There is significantly more load shed in the higher demand scenarios than the lower demand scenarios

(more than 5 MW) which results in higher $\text{CVaR}_{0.95}$ costs for the risk-neutral approaches.

The deterministic strategy produces less expected cost than the risk-neutral strategy. However, if the realized demand is the highest demand scenario, only committing Gen 1 in the second stage (as done in the deterministic problem) instead of both generators equates to nearly \$3,107 in total costs (last column of Table III) or an increase of \$15 in expected total economic costs. The \$15 reduction in expected total costs shows that there is a financial value added in considering the two-stage stochastic unit commitments over the deterministic problem.

2) *First stage 24hr representative day analysis:* The case when there are 11 active lines is analyzed for the full 24-hours for a representative day. Since the deterministic case only considers an expected demand with a maximum of 297 MW, which is less than the capacity of Gen 1, the second generator is not committed. Similar results were observed in Fig. 4(d). The results for the stochastic cases are shown in Figure 7(a)-(c) for the least demand scenario (scenario 1) and two highest demand scenarios (scenarios 4 and 5). In Fig. 7(a)-(c), the second generator is committed during the peak hours of the day (14-17 hours) and the corresponding time window is highlighted in green. Fig. 7(a)-(c) shows that the risk-averse cases tend to serve more demand during peak periods of the day than during hours of less demand as compared to the risk-neutral approaches. As discussed in Section III-C.1, the definition of $\text{CVaR}_{0.95}$ and the allocation of the same VoLL to each bus regardless of the location and time of day contribute to large drops in the three less costly first-stage demand scenarios for $\beta = 1$. The black dashed lines represent the demand corresponding to the five scenarios used in the optimization. Finally, for all the stochastic optimization strategies and the deterministic case, some portion of the expected total load is not served between hours 11 and 21.

3) *Second stage results:* In the second stage, the line de-energization and generator commitment decisions from the first stage are used to solve a 24 hour receding horizon optimization problem first for scenario 4 (S4) and then for scenario 5 (S5) as described in Section II-F2. The results are tabulated in Table 7. The risk-averse case has the lowest $\text{CVaR}_{0.95}$, but the demand served and total cost behavior varies as explained next. In scenario 4, the risk-averse case results in higher demand served (5,710 MWh) for lower cost (\$318,620) than the risk-neutral case (5,704 MWh, \$324,110). The opposite trend is observed for scenario 5 where the risk-averse case results in lower demand served (6,533 MWh) for higher cost (\$572,330) than the risk-neutral case (6,357 MWh, \$568,400). The deterministic case performed better than the risk-neutral approach in scenario 4 (5,704 MWh, \$324,050) since it does not activate Gen 2. However, in scenario 5, the deterministic performance (6,347 MWh, \$577,320) is more costly and serves less demand than the stochastic cases.

The demand served and lost load for scenario 5 are plotted in Fig. 7(d) and (e) respectively. The line energization decisions in the risk-neutral and deterministic cases are the same, but differ from the risk-averse case. Specifically, in the risk-averse case, the lines connected to bus 6 are not energized which results in the demand at that node being blacked out for

all hours of the day (Fig. 7(e)). The partially served demand at all buses (except bus 2, bus 3, and bus 6) is due to the power flow limit at line 2-5 which is reached from hours 12 to 20. Similarly, line 2-3 reaches its power flow limit at hour 16, affecting load delivery for bus 3. Over the entire time horizon, aside from the blackout at bus 6, buses 12 and 13 are the second and third most affected buses and lose nearly 16% and 13% of their total 24-hr load respectively. In the risk-neutral case, some portion of the demand is always served at all nodes. Buses 2, 4, 5, and 11 are at full service throughout the time horizon. Line 2-5 reaches its limit from hour 14 to 20 and line 2-3 in hour 16 resulting in unserved demand at bus 3. Buses 12 and 14 are the two most affected losing 34% and 32% of their total 24-hr load respectively. Since the deterministic case commits only Gen 1, the network cannot receive additional support from Gen 2 to serve buses 2 and 3 during hours 14 to 17 when line 2-5 reaches its maximum power flow capacity. Buses 2, 4, 6, and 10 had full service throughout the optimization horizon; however, buses 12 and 13 lost 70% and 44% of their total 24-hr load.

TABLE V: Demand served and cost of the second stage optimization with VoLL equal to 1,000 \$/MWh for Scenarios 4 and 5.

Risk averse (β)	S4 Dem. [MWh]	S4 Cost [\$]	S5 Dem. [MWh]	S5 Cost [\$]	$\text{CVaR}_{0.95}$ Cost [\$]
0.995-1	5,709.8	318,620	6,352.7	572,330	434,060
0-0.995	5,704.3	324,110	6,356.6	568,400	435,260
Deter.	5,704.3	324,050	6,347.0	577,320	439,290

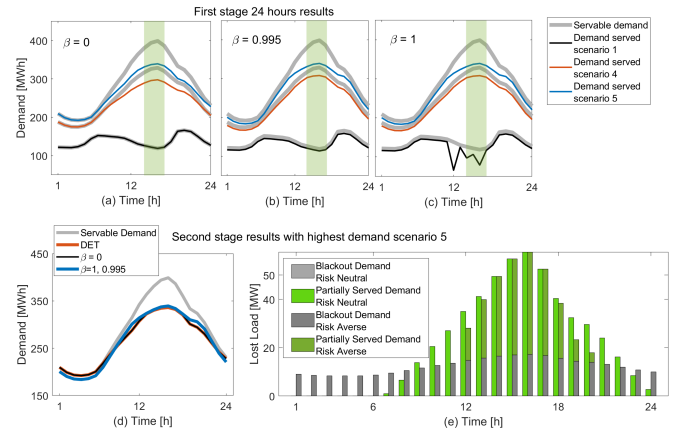


Fig. 7: All results are for 11 active lines at different risk averseness levels. Network-wide load served for demand scenarios 1, 4 and 5 for $\beta = 0$ (a), $\beta = 0.995$ (b), $\beta = 1$ (d). Green highlights the time window shows where Gen 2 is active. (d) Second-stage network-wide load served when the realized demand is the highest demand (scenario 5). (e) Types of load shed for the risk-neutral and risk-averse strategies as blackout demand or partially served demand.

IV. CONCLUSION

Both deterministic and stochastic frameworks are used to show how forecasts for high WFPI (that is often linked with occurrences of large wildfires) near transmission lines affect generator commitment and transmission line de-energization strategies. The proposed approach is implemented on the IEEE 14-bus test case and the optimal costs of commitment, operation, and lost load are compared to other public safety power shut-off models proposed in the literature. In general, our approach incurs less cost than previous methods that ignore economic costs, less system wildfire risks than planning methods unaware of wildfire risk, such as an $N-k$ approach, and it allows the operator to be more robust to changes in demand forecasts than deterministic approaches. Risk-averse decisions can be used by operators to reduce costs during high-demand periods of the wildfire season. However, additional studies may be needed to evaluate the fairness of blackouts that could result from risk-averse line de-energizations and the true costs of wildfire-related damages. Furthermore, the topology of the IEEE 14 bus system may not be the best representation of the grid in the portion of the United States under consideration. We plan to update our analysis with results from an N-1 secure WECC feeder.

REFERENCES

- [1] J. W. Muhs, M. Parvania and M. Shahidehpour, "Wildfire Risk Mitigation: A Paradigm Shift in Power Systems Planning and Operation," in *IEEE Open Access Journal of Power and Energy*, vol. 7, pp. 366-375, 2020, doi: 10.1109/OAJPE.2020.3030023.
- [2] A. Arab, A. Khodaei, R. Eskandarpour, M. P. Thompson and Y. Wei, "Three Lines of Defense for Wildfire Risk Management in Electric Power Grids: A Review," in *IEEE Access*, vol. 9, pp. 61577-61593, 2021, doi: 10.1109/ACCESS.2021.3074477.
- [3] California Public Utilities Commission. Public Safety Power Shut-off (PSPS)/De-Energization. Accessed: Oct. 2020. [Online]. Available: <https://www.cpuc.ca.gov/deenergization>
- [4] J. T. Abatzoglou, C. M. Smith, D. L. Swain, T. Ptak, and C. A. Kolden, "Population exposure to pre-emptive de-energization aimed at averting wildfires in Northern California," *Environ. Res. Lett.*, vol. 15, no. 9, Aug. 2020, Art. no. 094046.
- [5] "Climate Change Indicators: Wildfires." EPA, Environmental Protection Agency, <https://www.epa.gov/climate-indicators/climate-change-indicators-wildfires>.
- [6] "Number of Wildfires to Rise by 50 % by 2100 and Governments Are Not Prepared, Experts Warn." UN Environment, 23 Feb. 2022, <https://www.unep.org/news-and-stories/press-release/number-wildfires-rise-50-2100-and-governments-are-not-prepared>.
- [7] N. Rhodes, L. Ntairo and L. Roald, "Balancing Wildfire Risk and Power Outages Through Optimized Power Shut-Offs," in *IEEE Transactions on Power Systems*, vol. 36, no. 4, pp. 3118-3128, July 2021, doi: 10.1109/TPWRS.2020.3046796.
- [8] A. Kody, R. Piansky, and D. Molzahn, "Optimizing Transmission Infrastructure Investments to Support Line De-energization for Mitigating Wildfire Ignition Risk," in 11th Bulk Power Systems Dynamics and Control Symposium (IREP XI), Banff, Canada, July 2022.
- [9] N. Rhodes and C. Coffrin and L. Roald, "Security Constrained Optimal Power Shutoff", arXiv Preprint 2304.13778, 2023.
- [10] A. Kody, A. West, and D. Molzahn, "Sharing the Load: Considering Fairness in De-energization Scheduling to Mitigate Wildfire Ignition Risk using Rolling Optimization." Accessed: Oct. 24, 2022. [Online]. Available: <https://arxiv.org/pdf/2204.06543.pdf>
- [11] A. Umunnakwe, M. Parvania, H. Nguyen, and J. D. Horel, and K. R. Davis, "Data-driven spatio-temporal analysis of wildfire risk to power systems operation," 2021.
- [12] R. Bayani, M. Waseem, S. D. Manshadi and H. Davani, "Quantifying the Risk of Wildfire Ignition by Power Lines Under Extreme Weather Conditions," in *IEEE Systems Journal*, vol. 17, no. 1, pp. 1024-1034, March 2023, doi: 10.1109/JSYST.2022.3188300.
- [13] R. Moreno et al., "Microgrids Against Wildfires: Distributed Energy Resources Enhance System Resilience," in *IEEE Power and Energy Magazine*, vol. 20, no. 1, pp. 78-89, Jan.-Feb. 2022, doi: 10.1109/MPE.2021.3122772.
- [14] D. N. Trakas and N. D. Hatziaargyriou, "Optimal Distribution System Operation for Enhancing Resilience Against Wildfires," in *IEEE Transactions on Power Systems*, vol. 33, no. 2, pp. 2260-2271, March 2018, doi: 10.1109/TPWRS.2017.2733224.
- [15] Wildland Fire Potential Index (WFPI) Fire Danger Maps and Products Page, U.S. Geological Survey. (n.d.). <https://firedanger.cr.usgs.gov/apps/staticmaps>
- [16] D. Bienstock, A. Verma, "The N-k Problem in Power Grids: New Models, Formulations, and Numerical Experiments", *SIAM Journal on Optimization*, vol. 20, no. 5, pp. 2352-2380, 2010, doi = 10.1137/08073562X.
- [17] N. Gröwe-Kuska, H. Heitsch, and W. Römisch, "Scenario reduction and scenario tree construction for power management problems," in 2003 IEEE Bologna PowerTech - Conference Proceedings, 2003, vol. 3, pp. 152-158.
- [18] N. Noyan, "Risk-averse two-stage stochastic programming with an application to disaster management," *Computers & Operations Research*, vol. 39, no. 3, pp. 541-559, 2012. doi:10.1016/j.cor.2011.03.017
- [19] R. T. Rockafellar, S. Uryasev, "Optimization of Conditional Value at Risk," *Journal of Risk*, 2000, vol. 2, pp. 21-41.
- [20] M. Shaked, J.G. Shanthikumar, "Stochastic orders and their applications," Boston: AssociatedPress, 1994.
- [21] J. B. Rawlings, D. Q. Mayne, M. M. Diehl, "Model Predictive Control: The Theory, Computation, and Design 2nd Edition," Nob Hill Publishing, 2017, ISBN: 0975937731
- [22] "Reliability Test System Grid Modernization Lab Consortium (RTS-GMLC) Transmission System Database," Grid Modernization Lab, (2022). <https://github.com/GridMod/RTS-GMLC>
- [23] "OPF Case 14 Bus," Benchmark IEEE PES Power Grid Library for Optimal Power Flow v23.07, July 23, 2023; https://github.com/power-grid-lib/pglib-opf/blob/master/pglib_opf_case14_ieee.m
- [24] S. Mohagheghi and S. Rebennack, "Optimal resilient power grid operation during the course of a progressing wildfire," *Int. J. Elect. Power Energy Syst.*, vol. 73, pp. 843-852, 2015.
- [25] H. Farzin, M. Fotuhi-Firuzabad, and M. Moeini-Aghtaie, "Stochastic energy management of microgrids during unscheduled islanding period," *IEEE Trans. Ind. Informat.*, vol. 13, no. 3, pp. 1079-1087, Jun. 2017.
- [26] S. Sarykalin, G. Serraino, S. Uraysev, "value-at-Risk vs. Conditional Value-at-Risk Management and Optimization," *Tutorials in Operations Research*, 2008: 10.1287/educ.1080.0052